

A low-power, generic biostimulator with arbitrary pulse shape, based on a central control core

Milad Faizollah^{1a)}, Mousa Karimi¹, and Amir M. Sodagar^{1,2,3}

¹ Research Laboratory for Integrated Circuits and Systems (ICAS), ECE Dept., K. N. Toosi University of Technology, Tehran, Iran

² Polytechnique Montreal, Montreal, Quebec, Canada

³ School of Cognitive Sciences, Center for Research in Fundamental Sciences, Tehran, Iran

a) mfaizollah@m.ieice.org

Abstract: This paper reports on the design of a low-power biostimulator, capable of generating stimulus pulses with arbitrary wave shapes and programmable amplitude and timing. Designed based on a modular architecture with programmable stimulation details, this system can be used in a wide variety of applications. The system complies with basic requirements for biomedical stimulation systems such as small physical size, serial data communication with external setup, and low-power consumption. It also performs basic functions such as generating bi-phasic pulses, single/train pulses, and residual charge cancellation. Clock gating, operation with external timing, and shared resources are used among the main techniques to significantly reduce the power consumption of the system. To wirelessly interface with the external setup, a BPSK demodulator and clock recovery circuit is used which exhibit 100% data-rate-to-carrier-frequency ratio and consumes as low as 120 μW at 2.5 Mbps. The system was designed and simulated in a 0.18- μm standard CMOS technology, prototyped for functional verifications, and successfully tested.

Keywords: biostimulator, arbitrary waveforms, low-power

Classification: Electron devices, circuits, and systems

References

- [1] K. Chen, Z. Yang, L. Hoang, J. Weiland, M. Humayun, and W. Liu, "An integrated 256-channel epiretinal prosthesis," *IEEE J. Solid-State Circuits*, vol. 45, no. 9, pp. 1946–1956, Sept. 2010.
- [2] M. Zoladz, P. Kmon, P. Grybos, R. Szczygiel, R. Kleczek, and P. Otfinowski, "A bidirectional 64-channel neurochip for recording and stimulation neural network activity," *Proc. 5th Int. IEEE/EMBS Conf. Neural Eng.*, Cancun, Mexico, pp. 380–383, April–May 2011.
- [3] S. Ethier and M. Sawan, "Exponential current pulse generation for efficient very high-impedance multisite stimulation," *IEEE Trans. Biomed.*

- Circ. Syst.*, vol. 5, no. 1, pp. 30–38, Feb. 2011.
- [4] A. Wongsarnpigoon, J. P. Woock, and W. M. Grill, “Efficiency analysis of waveform shape for electrical excitation of nerve fibers,” *IEEE Trans. Neural Syst. Rehabil. Eng.*, vol. 18, no. 3, pp. 319–328, June 2010.
- [5] J. J. Sit and R. Sarpeshkar, “A low-power blocking-capacitor-free charge-balanced electrode-stimulator chip with less than 6 nA DC error for 1-mA full-scale stimulation,” *IEEE Trans. Biomed. Circ. Syst.*, vol. 1, no. 3, pp. 172–183, Sept. 2007.
- [6] M. Faizollah, “Design and implementation of a generic microcontroller for biomedical microsystems_ part1: the central core,” M.Sc. dissertation, K. N. Toosi Univ. of Tech., Dept. Elec. and Comp. Eng., Tehran, Iran, 2012.
- [7] M. Faizollah, S. Razmpour, A. M. Sodagar, M. Nourian, and M. Y. Darmani, “Low-power, small-size, generic controller dedicated to implantable biomedical microsystems,” *Proc. IEEE Biomed. Circ. Syst. Conference (BioCAS’ 12)*, Hsinchu, Taiwan, Nov. 2012.
- [8] F. Asgarian and A. M. Sodagar, “Wireless telemetry for implantable biomedical microsystems,” *Biomed. Eng., Trends in Elec., Comm. and Software*, ed. A. N. Laskovski, pp. 21–44, InTech, Croatia, 2011.

1 Introduction

For decades, electrical stimulation systems have been considered as potentially efficient tools for neurological and physiological studies as well as for clinical rehabilitation. Various biomedical stimulation devices such as cochlear implants, visual prostheses, pacemakers, deep brain stimulators (DBS), and spinal cord stimulators are developed to improve the quality of daily life for disabled people. Most of the recent stimulation systems use rectangular biphasic current waveform because of its simplicity [1, 2]. However, recently different other wave shapes for stimulation pulses are studied in order to increase the efficiency of stimulation [3]. Wave shape and timing parameters of stimulus pulses are believed to be among the key factors that contribute to the efficiency of stimulation [4].

In bi-phasic current pulses, any difference between the charges associated with anodic and cathodic pulses results in charge residual in the tissue which may result in tissue damage. To resolve this problem, several charge balancing circuits have been proposed to keep the accumulated charge below the safe level [1, 5]. These techniques are sometimes not welcomed because of the additional silicon area and power consumption they require.

To administer the operation of a biomedical microsystem, these devices usually comprise a digital controller. For this purpose, application-specific and commercial controllers are both used in these systems. A low-power and area-efficient generic controller has been recently developed by the authors for biomedical microsystems [6, 7]. This controller is capable of supporting a variety of applications such as recording and stimulation with fully programmable functional details.

As a necessity for a biomedical microsystem to be implanted inside the

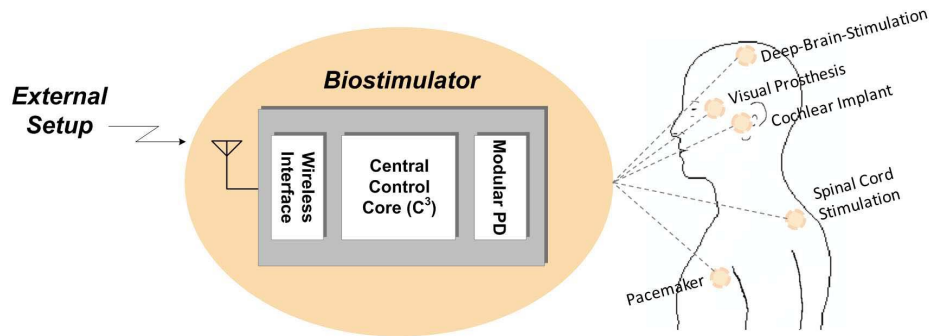


Fig. 1. The biostimulator block diagram.

body, it needs to exchange data with the external world through wireless connection [8]. Moreover, certain types of biomedical microsystems (*e.g.*, visual prostheses) require high data rate transfer from the external world to the implant part. As the energy loss in tissue increases by raising up the carrier frequency, maximizing the data-rate-to-carrier-frequency ratio for the wireless link helps transfer a large amount of data while keeping the carrier frequency as low as possible [8].

This paper introduces a generic stimulation system designed to be employed in a wide variety of rehabilitation applications as well as in advanced medical and biomedical research. The proposed bio-stimulator is capable of generating arbitrary pulse shapes with programmable amplitude and pulse width, and also canceling residual charges without any charge balancing circuitry. The system is designed with emphasis on efficient data exchange with the external setup, low-power consumption, and low-frequency operation.

2 System-level design

As shown in Fig. 1, in general, stimulus data and the power required for the operation of the system are wirelessly transferred from an external setup to the biostimulator. The central control core (C^3) processes the received data and sends the stimulus data to the peripheral device (PD), comprising data converters, storage devices, and tissue interface pieces such as microelectrode arrays. The proposed system relies on a continuous stream of operational information such as system setup, parameters, and system timing and also stimulation details from the external setup. This allows for the highest level of flexibility in generating arbitrary stimulus pulse shapes. This system is capable of generating mono-/bi-phasic pulses and the stimulation can occur between the electrode of interest and a reference electrode (mono-polar) or between any two electrodes (bi-polar).

3 The central control core (C^3)

As the heart of the biostimulator, the C^3 is in charge of decoding the incoming data packets, exchanging data between different blocks, controlling and administrating the operation of the whole system. The C^3 is the simplified version of the central core of the generic controller (reported in [6, 7]). Hard-

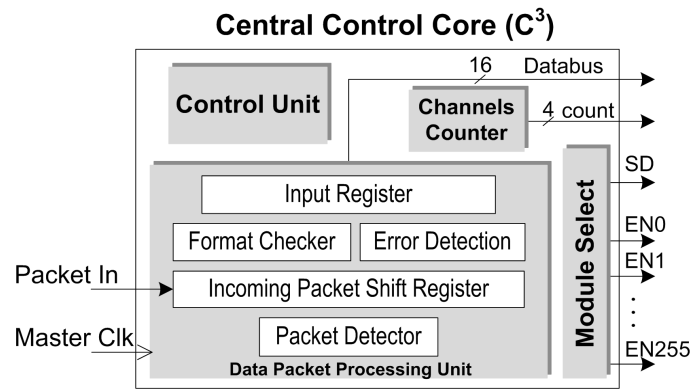


Fig. 2. Block diagram of the C^3 .

ware simplicity, programmability, serial data communication with external setup, and some power reduction techniques such as clock gating, hardware resources sharing, and operating at low clock frequencies are taken into consideration when designing this central core. Occupying $160\ \mu\text{m} \times 100\ \mu\text{m}$ of silicon area in a $0.13\text{-}\mu\text{m}$ standard CMOS technology, the central core consumes as low as $195\ \mu\text{W}$ in the stimulation mode. The C^3 and other digital parts in the proposed biostimulator, take advantage of the same architectural aspects and low-power design considerations as those used in the central core.

Block diagram of the C^3 is shown in Fig. 2. Data packets are transferred from the external setup to this system through an asynchronous serial wireless link. As shown in Fig. 3, each data packet starts with consecutive four logical 1's ("1111") for synchronization purposes. In applications where a huge amount of data is to be sent to the system in a fast and uninterrupted way, the *More Fragmented bit (MF)* is set to '1', meaning that the next similar data packets are received back to back and without start pulses. The *S/D* bit determines whether the received packet contains setup or status data of the stimulus pulses. *P0* and *P1* are even parity bits that accompany the information for error detection.

The *Data Packet Processing Unit* is responsible for detecting the data packets, checking the format of the received packets, detecting errors that are likely to happen during wireless data transmission, and sending the received data to their destinations (Fig. 2). All the timing and control signals needed for operation of different blocks are generated by *Control Unit*. The *Module Select* block, which can be programmed by the user, holds the address of the target modules.

Briefly, the C^3 receives the incoming data packets along with a synchronous clock (clock frequency = 2.5 MHz) from the wireless interface. The

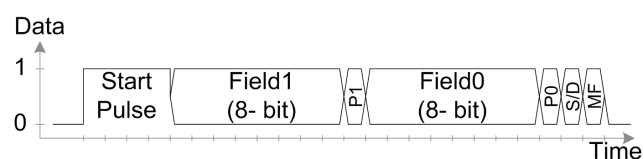


Fig. 3. The data packet format.

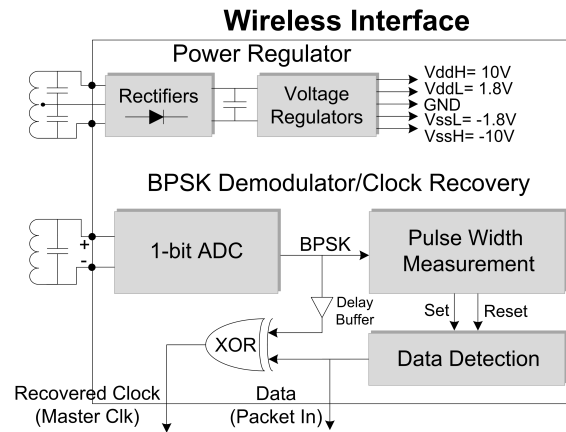


Fig. 4. Block diagram of the wireless interface.

received data packets are processed by the C^3 and the stimulus data are then sent to the PD.

4 Biostimulator interfaces

As illustrated in Fig. 1, the system interfaces with both the external setup and the body using the wireless interface and the modular PD, respectively. More details will be provided in the proceeding sub-sections.

4.1 The wireless interface

The wireless interface module is in charge of retrieving power, data, and clock from the received signal through the wireless link. The recovered data and clock will be used by the C^3 and the power will be distributed throughout the entire system. Fig. 4 shows a simplified block diagram for the wireless interface module of the system. Reaching high power-transmission efficiency, high data-transmission bandwidth, and coupling insensitivity, both power and data are transferred wirelessly through two separate inductive links. The *Power Regulator* block, consisting of an LC-tank, a voltage rectifier, and a set of voltage regulators, generates $\pm 10\text{ V}$ and $\pm 1.8\text{ V}$ supply voltages.

For the wireless transmission of data toward the system it is binary phase shift keying (BPSK) modulated. The BPSK demodulator used in this work consumes as low as $120\ \mu\text{W}$ from a 1.8 V supply at the data rate of 2.5 Mbps . Besides the low power consumption and circuit simplicity of this demodulator, it is capable of exhibiting a data-rate-to-carrier-frequency ratio of as high as 100%. The BPSK demodulator also recovers a clock synchronized with the retrieved data from the signal received through the wireless link.

The analog signal received through the wireless link, it is first digitized using a *1-bit* ADC, realized using a Schmitt trigger circuit. As shown in Fig. 5, the result is a stream of binary pulses whose widths are determined by the binary information with it. The pulses at the output of the *1-bit* ADC (the BPSK signal) are of twice width when a data transition occurs in the data stream (Fig. 5). A wide High pulse (HI) corresponds to a Low-High data transition and a wide Low pulse (LO) corresponds to a High-Low

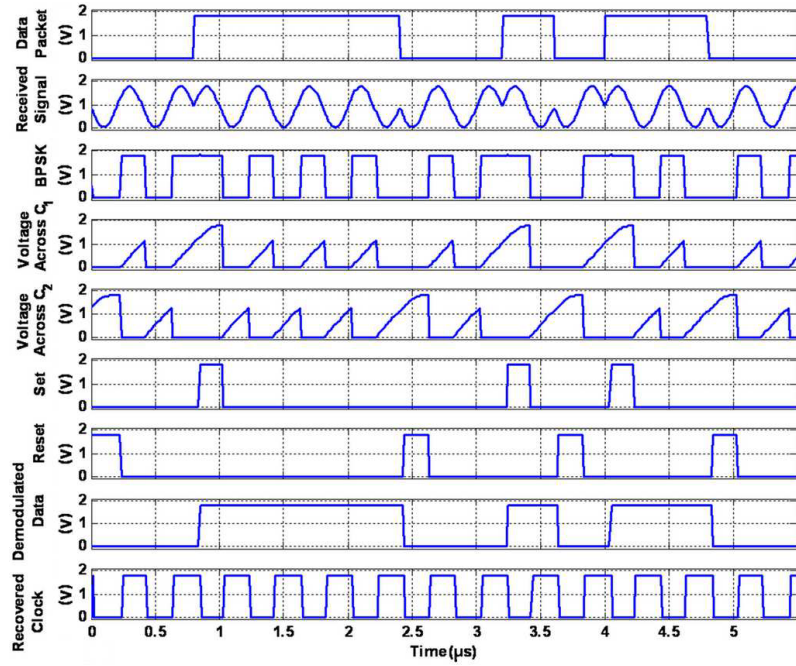


Fig. 5. Simulated waveforms of the BPSK demodulator.

transition. Therefore, to retrieve the received bit stream, one needs to detect the wide pulses (both HI and LO). Fig. 6 shows the schematic diagram of the *Pulse Width Measurement (PWM)* block. In the *PWM* block, to discriminate wide pulses from the narrow ones, capacitors C_1 and C_2 are charged using the constant current sources I_1 and I_2 , respectively. C_1 is charged during the presence of a HI pulse. It is only for wide HI pulses that the output of Schmitt trigger1 (*Set* signal) goes high. *Reset* signal in Fig. 6 is activated with the same mechanism when a wide LO pulse occurs. The *Set* and *Reset* signals are then delivered to an SR-latch in *Data Detection* block in order to retrieve the data received from the outside.

In addition to data detection, the proposed circuit is also capable of recovering a clock signal synchronized with the detected data. It can be shown that this synchronized clock can be recovered by Exclusive-ORing the BPSK signal and the detected data.

It is worth noting that although one of the input signals of XOR gate passes the *PWM* and *Data Detection* blocks which seems to have more delay,

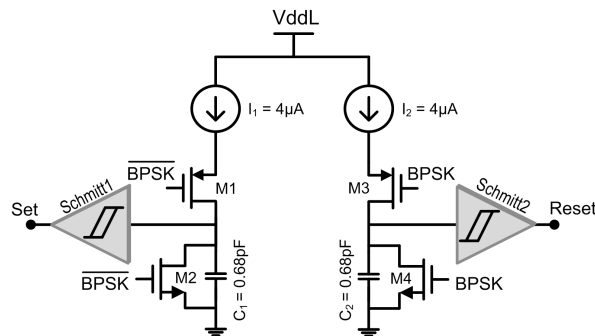


Fig. 6. Schematic diagram of the *Pulse Width Measurement* block.

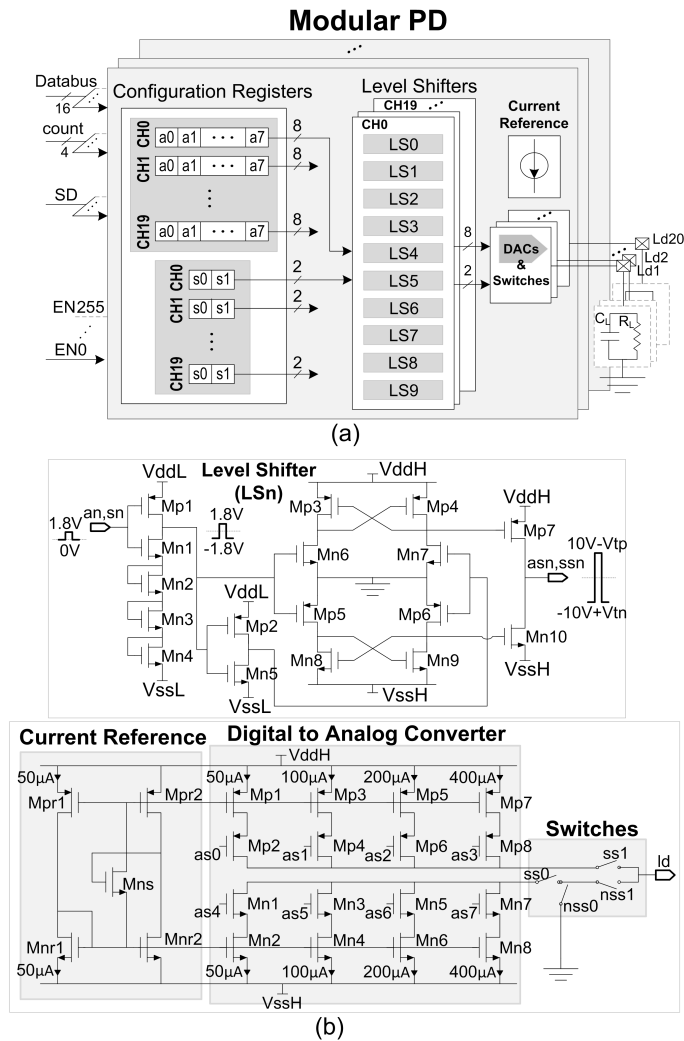


Fig. 7. (a) Block diagram of the modular PD, (b) the stimulation back-end.

because of the simplicity of these blocks the delay is too small and can be neglected. However, as shown in Fig. 4, a buffer is used to delay the BPSK signal in order to compensate for this delay.

4.2 The modular PD

As illustrated in Fig. 7(a), the biostimulator has a modular architecture. Sharing the C^3 , the wireless interface, and a current reference between all the modules of the system, physical size and power consumption of the system are reduced.

Each module is capable of driving up to 20 stimulating electrodes and the C^3 is capable of addressing up to 256 modules which is appropriate for high-density stimulation applications (*e.g.*, visual prostheses). The amount of current injected into tissue and the status of each electrode (high impedance, grounded or connected to either anodic or cathodic current path) are carried by the received data packets. An 8-bit stimulus amplitude and a 2-bit pulse status word for each channel are stored in the *Configuration Registers* block, as shown in Fig. 7(a). To have a high amount of current injected to the load,

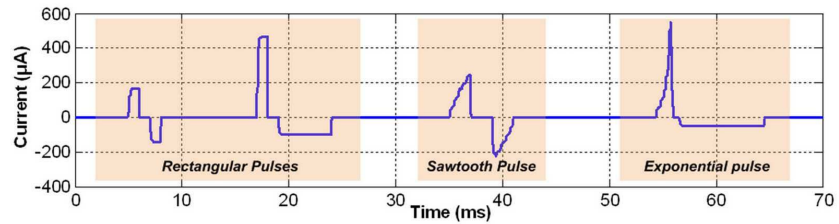


Fig. 8. Simulation results of the stimulation back-end for a single electrode.

outputs of the *Configuration Registers* are connected to the *Level Shifters* (LS_n). Detailed circuit schematic for the stimulation back-end is shown in Fig. 7 (b). In this circuit the LS_n shifts the voltage levels from (0-1.8 V) to ± 10 V. For each channel, shifted voltages of an 8-bit stimulus amplitude and a 2-bit pulse status registers are conveyed to a pair of 4-bit digital to analog converters (DAC) and switches, respectively.

Moreover, for the sake of safety, each channel is shorted after injecting a bi-phasic stimulus pulse in order to cancel any residual charges.

Fig. 8 shows the simulated operation of the stimulation back-end in a $0.18\text{-}\mu\text{m}$ standard CMOS technology. In the simulation, the system is operated to generate stimulation pulses with three different wave shapes. First, two rectangular pulses with different amplitude and pulse duration are generated. Then a bi-phasic sawtooth pulse follows. Finally, a stimulation pulse with rising exponential shape for the anodic part and a rectangular low-amplitude cathodic pulse is generated to show the flexibility of the operation of the system in the case of arbitrary pulse shapes. Time specifications of the stimulation pulses (anodic and cathodic pulse widths as well as the interface delay) can be defined with a resolution of as fine as around $9\ \mu\text{s}$.

5 Power reduction techniques

To lower the power consumption of the biostimulator, three specific techniques have been taken into consideration:

- To reduce the dynamic power consumption of the biostimulator ($P_{dyn} = \alpha_T \cdot C_{load} \cdot V_{dd}^2 \cdot f_{clk}$), clock signal for the parts of the system that are inactive for periods of time, is gated.
- The system operates with external timing, complex processing tasks are performed in the external setup, and the 100% data-rate-to-carrier-frequency ratio of BPSK demodulator allow the system to operate at reasonably low clock rates.
- Modular architecture of the system and sharing some hardware resources also help reduce the power consumed by the system.

Simulating the system in a $0.18\text{-}\mu\text{m}$ standard CMOS technology, a benchmark is developed to estimate power consumption of the biostimulator. Running the benchmark, random data are generated to estimate the average power consumption for different blocks of this system (Fig. 9). As a result

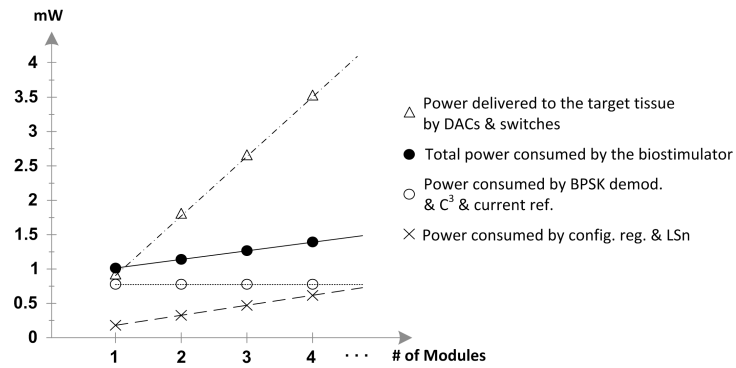


Fig. 9. Power distribution in the biostimulator.

of employing the power reduction techniques, for 4 modules and more, the power consumed by the system is much lower than the power delivered to the target tissue for stimulation. It is worth noting that unlike the power delivered to the target tissue, which increases proportionally with the number of modules, the power consumed by the system itself increase slightly as more modules are used.

6 Experimental prototyping and results

Fig. 10(a) shows the experimental setup of the system for single-channel stimulation. To evaluate the functionality of the biostimulator system re-

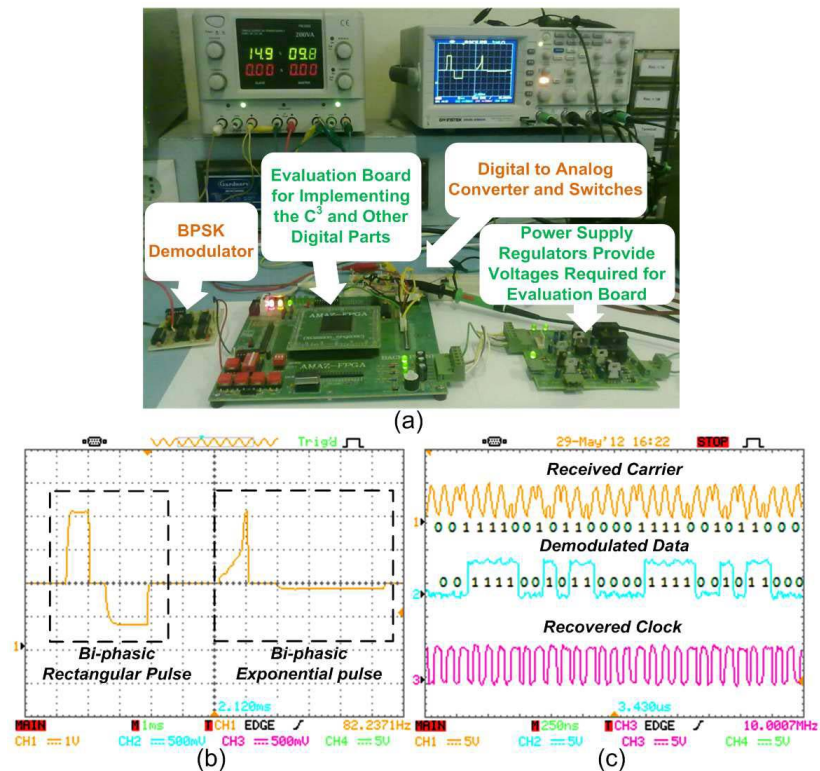


Fig. 10. The biostimulator experiments, (a) experimental setup, (b) operation of the biostimulator, (c) the BPSK demodulator operation.

ported in this paper, the C^3 and other digital blocks were implemented on an FPGA and the rest of the system was prototyped using off-the-shelf components and functionally-equivalent commercial ICs. In fact, it is not feasible to implement the proposed analog circuits designed in the transistor-level (e.g., the DAC) using off-the-shelf components. However, to test the functionality of the whole system, functionally-equivalent commercial ICs were used for those analog circuits. Therefore, four least-significant input bits of the commercially-available DAC (DAC0808) were used and 74HC4066 quad-analog-switch ICs were employed to realize the equivalent function of the proposed stimulation back-end circuit. Oscilloscope screen shots demonstrating the operation of the system and that of the BPSK demodulator are shown in Fig. 10 (b) and (c), respectively.

7 Conclusion

A low-power generic stimulation system is introduced, which is capable of generating arbitrary waveforms supporting a variety of implantable biomedical applications. To reduce power consumption of the system, some techniques such as clock gating, external timing operation, and resource sharing are used. In addition, employing a low-power BPSK demodulator with 100% data-rate-to-carrier-frequency ratio results in the operation of the system at considerable low clock frequency. The system was simulated, prototyped, and tested successfully.